

The run-up of weakly-two-dimensional solitary pulses

M. Brocchini

Istituto di Idraulica, Università di Genova, Via Montallegro 1, 16145 Genova, Italy

Received: 20 April 1998 – Accepted: 18 May 1998

Abstract. The run-up of solitary-type pulses propagating at a small angle with respect to the shore normal is analysed by means of a weakly-two-dimensional extension of a solution of the nonlinear shallow water equations for a non-breaking, solitary pulse incident and reflecting on an inclined plane beach similar to that of Synolakis (1987). A simple analytic expression for the longshore velocity of the solitary-type pulse is given along with examples of computations. The proposed solution can be employed in modelling run-up flow properties of solitary-type pulses (e.g. *tsunamis*, primary waves of wave groups propagating in shallow waters, ...). The hodograph transformation that is used and the flow properties are illustrated in terms of contour plots. A limiting pulse amplitude is defined such that breakdown of the solution occurs. A solution for the run-up of multiple-solitary-pulses in shallow waters is also described. Some of the salient characteristics are illustrated and discussed. Breakdown conditions are analytically defined also for the multiple-solitary-pulses solution. A strong condition is given which couples information on both pulses amplitudes and distances. An easier (but weaker) version of the criterion is given in terms of a pair of decoupled formulae one for the pulses amplitudes and the second for their initial positions. Very large run-up is achieved because of the merging of two or more solitary pulses which are smaller than the limiting pulse. The role of pulse separation within a group of solitary pulses is also analysed in terms of both a 'nonlinearity parameter' \mathcal{N} and a 'groupiness parameter' \mathcal{G} . It is found that a critical distance exists between two pulses which minimizes the back-wash velocity and, as a consequence, the nonlinearity parameter \mathcal{N} .

1 Introduction

The motion of water waves near the shoreline on a gently sloping beach has been described by many authors using var-

ious hydrodynamical equations: linear and nonlinear shallow water equations, Boussinesq and various approximations to these equations. A long-wave approximation for the full equations of motion gives as the leading terms (e.g. Peregrine, 1972) the nonlinear shallow water equations (NLSWE). These equations are obtained by assuming that vertical accelerations of the water, or those normal to the beach, are negligible compared with gravity. The same sort of equations can be successfully used to model the run-up of *tsunamis* which are long waves generated either by submarine tectonic displacements, or landslides (see for example Carrier (1966)). These are essentially waves propagating in shallow waters.

Carrier and Greenspan (1958) (hereinafter CG) give an analytical solution for the shallow-water motion of temporally periodic, finite amplitude, non-breaking standing waves on a beach of constant slope. It is still one of the few analytical solutions available, together with that derived by Shen and Meyer (1963) for run-up due to a bore. A third analytical solution is that by Synolakis (1987) (hereinafter SY87) in which a solitary-type pulse is used as an initial condition for the NLSWE. At present, Synolakis' solution is, although not of permanent form, the only NLSWE analytical solution for the run-up of solitary pulses which includes the effects of reflection and has proved very successful in predicting inundation patterns of solitary waves.

All the above analytical solutions are attractive as they allow direct computation of flow properties in the near-shore region. They also represent 'benchmarks' for comparing and testing any numerical solver of the NLSWE. However, their drawback rests in their horizontal one-dimensional nature. This together with the calculation of the velocity characteristics in the waves run-up have been considered as the main unsolved problems related to *tsunamis* run-up (see Voit (1987)). Hence, the relevance of the present work to the study of *tsunamis* run-up.

A few cases of studies of the evolution of horizontally-two-dimensional long waves can be found in the literature. For example the work of Carrier and Noiseux (1983) deals

with the interaction of tsunamis waves with a coastline. They compute the reflection of obliquely incident tsunamis off a continental shelf. Characteristics of the reflected waves and of the run-up are studied by solving the linear shallow-water equations. A second work can be mentioned by Golinko and Pelinovsky (1988) which refers to the run-up of long waves in a channel of arbitrary cross-section.

Recently Brocchini and Peregrine (1996) (hereinafter BP) extended the finite amplitude, standing-waves solution by CG for the case of weakly-two-dimensional periodic flow conditions. This new solution was used to discuss the water flow in the 'swash zone' i.e. in that part of a beach over which the instantaneous shoreline moves back and forth as waves meet the shore.

Although very useful to model periodic flow conditions, that solution cannot be used to represent those flow conditions in which a single wave group propagates, with a small angle to the beach normal, from deep waters into shallow waters. Examples of evolution of an envelope soliton (solution of the nonlinear Schrödinger equation) from deep to shallow waters have been numerically analysed by Barnes and Peregrine (1995). Some of their computations suggest the group in shallow waters can be represented as made of primary waves behaving like solitary waves and a wave of depression.

During the time that a wave group is in the swash zone, there is a complex interaction between the waves in the group and the swash motion from previous waves. These are thought to be critical in assessing the generation properties of low frequency waves in the swash zone (Watson, Barnes and Peregrine (1994)). Hence, the need for a solution for N solitary waves interacting in shallow waters.

In section §2 a solution is therefore proposed along with some test case which enables analytical computation of all the main flow properties (free water surface and both velocity components) associated with the run-up of weakly-two-dimensional solitary pulses. A novel analytical solution is also given in section §3 for interacting solitary pulses in shallow waters (multiple-solitary-pulses solution). The main examples of application of the above solutions are both the run-up of a single group of waves (multiple solitary waves) and the run-up of a tsunamis (single solitary wave). Both solutions are characterised within their domain of validity i.e. providing breakdown does not occur. A summary of the results is given in section §4 along with some considerations on ongoing and future research.

2 A weakly-two-dimensional solitary pulse solution

In the following we briefly introduce the mathematical background used to compute the solution. This is also characterized by means of a couple of relevant test cases.

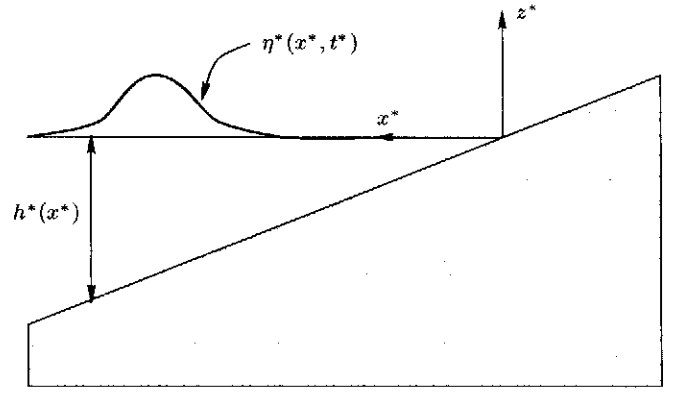


Fig. 1. Flow and coordinates definition.

2.1 Theory and background

Using dimensional (starred) variables we introduce basic definitions (see figure 1) choosing the still water level to be $z^* = 0$ and the total water depth:

$$d^*(x^*, y^*, t^*) = h^*(x^*) + \eta^*(x^*, y^*, t^*) \quad (2.1)$$

where $z^* = h^*(x^*)$ is the seabed, and $z^* = \eta^*(x^*, y^*, t^*)$ is the position of the free surface. Thus, the x^* -coordinate is pointing seaward i.e. here we use a convention opposite to that used by CG and BP.

For a plane beach, the equations without bottom friction can be put in a simple dimensionless form with no explicit dependence on the beach slope (e.g. Meyer and Taylor, 1972; Brocchini and Peregrine, 1996). According to the scaling used in CG and BP it is:

$$x = \frac{x^*}{l_0}; \quad y = \frac{y^*}{l_0}; \quad t = \frac{t^*}{[l_0/(g\theta)]^{1/2}} \quad (2.2a)$$

$$d = \frac{d^*}{d_0} = \frac{d^*}{\theta l_0}; \quad L = \frac{L^*}{l_0}; \quad u = \frac{u^*}{(gl_0\theta)^{1/2}}; \quad v = \frac{v^*}{(gl_0\theta)^{1/2}} \quad (2.2b)$$

where d_0 and l_0 are the two scales respectively used for vertical and horizontal lengths and θ [$\mathcal{O}(10^{-3})$ typically] is the angle between the horizontal and the beach face. Hence the dimensionless (unstarred) equations read:

$$d_t + (ud)_x + (vd)_y = 0 \quad (2.3a)$$

$$u_t + uu_x + vv_y + d_x = 1 \quad (2.3b)$$

$$v_t + uv_x + vv_y + d_y = 0 \quad (2.3c)$$

where u and v are respectively the depth-averaged onshore and longshore velocity components and where the right hand side of each equation represents the 'beach source term' (i.e. the acceleration due to the beach slope in (b) and (c)).

Equations (2.3) can be further simplified by approximating for waves incident at small angle to the beach normal and for weakly-two-dimensional flow (Ryrie, 1983). The fully coupled set of equations can be decoupled in a set of two equations in characteristic form for the 'onshore problem'

$$\alpha_t + (u + c)\alpha_x = 0 \quad (2.4a)$$

$$\beta_t + (u - c)\beta_x = 0 \quad (2.4b)$$

and one for the 'longshore problem':

$$\gamma_t + u\gamma_x = 0. \quad (2.5)$$

The Riemann invariants α , β and γ depend on the 'beach term' and they are:

$$\alpha = 2c + u - t \quad (2.6a)$$

$$\beta = 2c - u + t \quad (2.6b)$$

$$\gamma = v - \frac{1}{2}u^2 - d + x = v - \frac{1}{2}u^2 - \eta. \quad (2.6c)$$

CG used a hodograph transformation in solving the 'onshore problem':

$$\lambda = \alpha - \beta = 2(u - t) \quad (2.7a)$$

$$\sigma = \alpha + \beta = 4c \quad (2.7b)$$

$$u(\sigma, \lambda) = \frac{\phi_\sigma}{\sigma}. \quad (2.7c)$$

Using the above transformation the two characteristic equations for the 'onshore problem' can be combined to give a *single linear equation* in ϕ :

$$(\sigma\phi_\sigma)_\sigma - \sigma\phi_{\lambda\lambda} = 0. \quad (2.8)$$

Finally the usual (x, t) coordinates are related to (σ, λ) as follows:

$$x = \frac{1}{16}\sigma^2 - \frac{1}{4}\phi_\lambda + \frac{1}{2}u^2 = \frac{1}{16}\sigma^2 - \eta \quad (2.9a)$$

$$t = \frac{\phi_\sigma}{\sigma} - \frac{1}{2}\lambda. \quad (2.9b)$$

Following BP we now solve the 'longshore problem' and give an analytical solution for the longshore velocity v . Therefore we integrate equation (2.5) using the CG coordinate transformation. After some non-trivial algebra the equation can be rearranged to give:

$$\left(\frac{\phi_{\sigma\lambda}}{\sigma} - \frac{1}{2}\right)\left(2v_\lambda - \frac{\phi_\sigma}{\sigma}\right) + \frac{1}{2}\left(\phi_{\sigma\sigma} - \frac{\phi_\sigma}{\sigma}\right)\left(\frac{1}{2} - \frac{4v_\sigma}{\sigma}\right) = 0. \quad (2.10)$$

A solution valid for any ϕ is

$$v = \frac{1}{4}\phi_\lambda. \quad (2.11)$$

This solution has been used by BP to extend CG standing-wave solution for weakly-two-dimensional flow conditions. In a similar fashion we use (2.11) to extend a solitary pulse solution similar to that found by Synolakis. We refer to SY87 for most of the details on the mathematical derivation of the solution and report here only the main results.

Equation (2.8) is solved by means of a Fourier transform technique. It can be shown that a suitable solution which is bounded at the shoreline $\sigma = 0$ and at $\sigma = \infty$ takes the form (in our dimensionless and scaled variables):

$$\phi(\sigma, \lambda) = -16i \int_{-\infty}^{\infty} \frac{\Phi(k)}{k} \frac{J_0(k\sigma/2)e^{-ik(1-\lambda/2)}}{J_0(2k) - iJ_1(2k)} dk \quad (2.12)$$

where J_0 and J_1 are the Bessel functions of order zero and one respectively. The particular form of the solution is specified by $\Phi(k)$. For a solitary pulse centered at $x = X$ at $t = 0$ the following profile is here used:

$$\eta(x, 0) = A \operatorname{sech}^2 \xi(x - X) \quad (2.13)$$

where A is the dimensionless pulse height and $\xi = (3A/4)^{1/2}$. Please note that A corresponds to the height-to-depth ratio of Synolakis' solution and comparison of the results is made accordingly.

The transform function $\Phi(k)$ associated with the profile is:

$$\Phi(k) = \frac{2}{3}k \operatorname{cosech}(\beta k) e^{ikX} \quad (2.14)$$

where $\beta = \pi/2\xi$. On substitution into equation (2.12), we obtain the specific solution for a single solitary pulse as:

$$\phi = -\frac{32i}{3} \int_{-\infty}^{\infty} \operatorname{cosech}(\beta k) \frac{J_0(k\sigma/2)e^{ik\vartheta}}{J_0(2k) - iJ_1(2k)} dk \quad (2.15)$$

where $\vartheta = X - 1 + \lambda/2$.

We are now able to compute explicitly all the flow variables by inserting the above solution in (2.7c), (2.9) and (2.11):

$$u = \frac{16i}{3} \int_{-\infty}^{\infty} k \operatorname{cosech}(\beta k) \frac{J_1(k\sigma/2)e^{ik\vartheta}}{\sigma[J_0(2k) - iJ_1(2k)]} dk \quad (2.16a)$$

$$v = \frac{4}{3} \int_{-\infty}^{\infty} k \operatorname{cosech}(\beta k) \frac{J_0(k\sigma/2)e^{ik\vartheta}}{J_0(2k) - iJ_1(2k)} dk \quad (2.16b)$$

$$\eta = v - \frac{1}{2}u^2. \quad (2.16c)$$

These properties can be computed either by direct integration or by using Cauchy's integral formula. In SY87, the Laurent series for the above integrals are computed together with the related asymptotic expansions for large values of σ and ξ .

In order to illustrate the behaviour of (u, v, η) and avoid troubles with any eventual singularities in the $(\sigma, \lambda) \rightarrow (x, t)$ transformation, we prefer to perform a direct numerical computation of the integrals and constantly monitor the behaviour of the Jacobian

$$\mathcal{J} = c \left[u_\sigma^2 - \left(u_\lambda - \frac{1}{2} \right)^2 \right]. \quad (2.17)$$

Convergence is ensured by performing the integration over the $(-5, 5)$ range for k using a constant integration step of $dk = 0.001$ (Synolakis, private communication).

2.2 Two cases of single pulses

We now illustrate the main flow characteristics referring to two specific examples. In particular we discuss the patterns of the free surface elevation, of the onshore velocity u and of the longshore velocity v . Furthermore, it is interesting to visually inspect the hodograph transformation of $(\sigma, \lambda) \rightarrow (x, t)$. This is an alternative approach to that which employs plots of characteristic curves to inspect the dynamics of the flow. We find this alternative method more useful for the case in hand because characteristics are useful for determining bore initiation far from the shoreline. Here breakdown occurs close to the shoreline. Another advantage of analysing the hodograph transformation is to relate the point of breakdown of the solution to the coordinates mapping.

Table 1. Equivalent wave length of solitary pulses

Amplitude (A)	Length (L)
0.81	2.8
0.70	3.0
0.60	3.3
0.50	3.7
0.25	5.0

The first example refers to a solitary pulse characterized by $A = 0.5$ and $X = 4$. The choice of the amplitude, which for the case of a single pulse is only of practical convenience, has been made in view of the multiple-solitary-pulses discussed in the next section. On the other hand the distance X from the still water shoreline has been chosen in dependence of the ‘reference length’ or ‘equivalent pulse length’ L of the solitary pulse.

It is common to define an ‘equivalent wave length’ L in the sense of the distance within which the surface elevation exceeds some (p) percent of its maximum value i.e. such that

$$\eta(L) = pA. \quad (2.18)$$

This definition can be specified by using solution (2.13) and choosing $p = 0.05$. After SY87 this measure became a standard length used for solitary waves (see also Kobayashi, DeSilva and Watson (1989)) and is defined as:

$$L = (1/\xi) \operatorname{arccosh} \left(\sqrt{\frac{1}{0.05}} \right). \quad (2.19)$$

We immediately see that this length decreases with the amplitude A . A few reference values of L are reported in table 1 for the cases under investigation. Note that it is not correct to use the dimensionless variables d and L to define a condition on the suitability of the NLSWE rather it is necessary to use the dimensional variables d^* and L^* .

According to the scaling (2.2), the relation for the dimensional variables reads:

$$\frac{d^*}{L^*} = \theta \frac{d}{L} \quad (2.20)$$

giving

$$d^*/L^* = \mathcal{O}(\theta) \ll 1 \text{ and } U_r = \frac{A^*}{k^{*2} d^{*3}} = \mathcal{O} \left(\frac{1}{\theta^2} \right) \gg 1. \quad (2.21)$$

for $d/L = \mathcal{O}(1)$ and $A/d = \mathcal{O}(1)$ which are typical values used in our analysis (here U_r represents the Ursell number).

The location X of the pulse centre (where $\eta = A$) is about a distance L offshore of the limit $X_0 = 1$ of the ‘shallow water region’, where the value of X_0 is defined by requiring that offshore of it nonlinear contributions in both (2.9) and (2.16) can be neglected (e.g. Carrier (1966)). Hence we define:

$$X = X_0 + L = 1 + L. \quad (2.22)$$

Inspection of table 1 reveals that appropriate distances for pulses of amplitude conditions $0.50 \leq A \leq 0.81$ is in the

range $3.8 \leq X \leq 4.7$. We therefore choose a value for the distance $X = 4$ which is approximately valid for most considered pulse conditions and is near exact for the pulse of limiting amplitude which, in the following analysis, is used as ‘benchmark’.

For the case in hand the relevant contour plots are reported in figure 2. Inspection of figures 2(a) and 2(c) shows that a very similar pattern characterizes the free surface elevation η and the longshore velocity v : the contours $\eta = v = 0.34$ and $\eta = v = 0.47$ represent a pair of ‘ridges’ in the (x, t) plane. These ‘ridges’ are produced by the solitary pulse which propagates from the seaward boundary of the domain and is reflected at the shore. Taking a ‘slice’ at a fixed value of the x -coordinate means we are following the time evolution of the signal. For example, the profile of the free surface elevation η at $x = 3$ only shows the peak of the incident signal for $t < 3$. However, for $t > 6$ peaks of both the incident and a reflected signal are present. These signals are separated by ‘shelf’ region which has been experimentally observed.

Although very similar away from the shoreline, the patterns of η and v become rather different close to the undisturbed shoreline. Differences are due to the nonlinear term $u^2/2$ which appears in (2.16c). This becomes non-negligible only for small values of x . This can be quantified by introducing a measure of the intensity of nonlinearities as

$$\mathcal{N} = \frac{\operatorname{Max}(\eta - v)}{\operatorname{Max}(\eta)} = \frac{\operatorname{Max}(u^2/2)}{\operatorname{Max}(\eta)}. \quad (2.23)$$

For the present case it is $\mathcal{N} \approx 0.40$. \mathcal{N} is used more extensively in the next section for analysing merging pulse i.e. multiple-solitary-pulses.

A completely different pattern is seen in figure 2b for the onshore velocity component u . This is essentially antisymmetric with respect to the time when the maximum run-up is reached. At this time both η and v reach their maximum value which, due to the antisymmetric structure of u and to equation (2.16c), is the same:

$$\operatorname{Max}(\eta) = \operatorname{Max}(v). \quad (2.24)$$

Note also that because of the particular choice of coordinates (i.e. the x -axis pointing seaward) the velocity of the incident pulse is negative as $dx/dt < 0$.

Figure 2d illustrates the behaviour of the (σ, λ) coordinates in the (x, t) plane. Breakdown is caused by singularities of the Jacobian \mathcal{J} and is shown by the strong deformation of the coordinate grid. This could be interpreted in terms of wave breaking where the flow becomes turbulent. However, Meyer suggests that wave breaking should not be confused with the breakdown of the coordinate transformation (Liu, Synolakis and Yeh, 1991). In the following we therefore refer to a ‘solution breakdown’ rather than to ‘wave breaking’.

In the specific example of figure 2d, breakdown occurs during the back-wash phase and is indicated by the arrow. Here the (σ, λ) coordinate grid becomes highly distorted and the $(\sigma, \lambda) \rightarrow (x, t)$ transformation is no longer single valued. The restriction for breakdown during the back-wash is

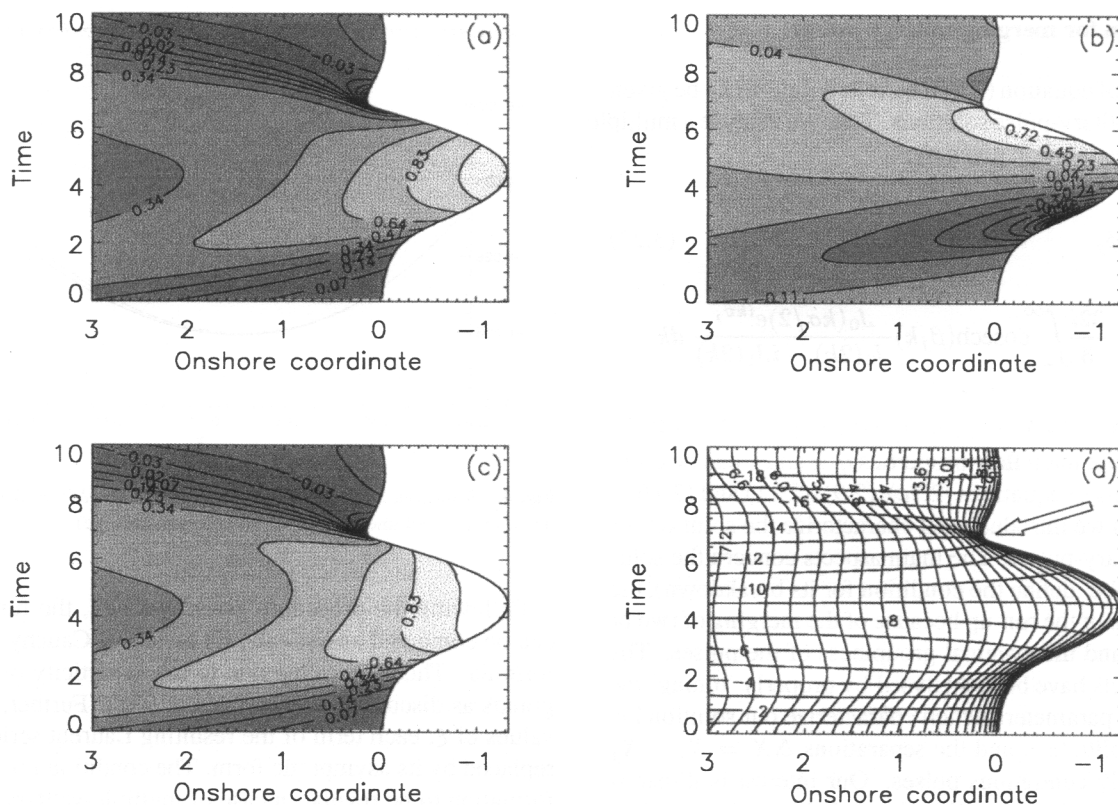


Fig. 2. Solitary pulse as for (2.14) with $A = 0.5$ and $X = 4$. Contour lines of: (a) the free surface elevation η , (b) the onshore velocity component u , (c) the longshore velocity v and (d) the (σ, λ) -coordinates in the (x, t) -plane. Lines of constant λ run from left to right whilst lines of constant σ run from top to bottom. Breakdown occurs only during the back-wash and it is indicated by the arrow. Contour values increase from dark blue to white.

weaker than for the e.g. SY87). From a physical point of view this means that waves that do not break during the run-up may break during the back-wash.

In the following, however, we only discuss the breakdown of the solution during the pulse run-up. In order to establish the conditions of breakdown we performed a large number of numerical computations using pulses of different heights. It is found that breakdown occurs for pulse of dimensionless height such that:

$$A > 0.81. \quad (2.25)$$

This criterion essentially confirms that obtained by Synolakis: by means of an asymptotic analysis he computed a limiting height-to-depth ratio of 0.81

Again breakdown of the solution is clearly illustrated by representing the contour plots of the hodograph transformation for a solitary pulse of $A = 0.81$. The arrow in figure 3 indicates the region where the coordinate grid is distorted because of breakdown during the pulse run-up. Clearly the back-wash, occurring for $t > 4.5$, is characterized by an even stronger distortion of the coordinate grid.

A final result achieved by numerically integrating the solution rather than relying on asymptotic expansions concerns the maximum run-up which can be easily computed by the

expression

$$\mathcal{R} = 3.11 A^{5/4} \quad (2.26)$$

where $\mathcal{R} \equiv |x_{min}|$. Although the dependence of the run-up on the pulse amplitude confirms that given by Synolakis the numerical coefficient obtained by numerical integration is slightly larger (Synolakis computed a value of 2.83).

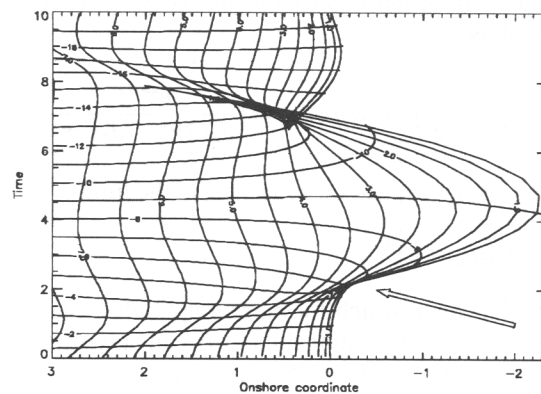


Fig. 3. Solitary pulse as for (2.14) with $A = 0.81$ and $X = 4$. Contour lines of the (σ, λ) -coordinates in the (x, t) -plane. Lines of constant λ run from left to right whilst lines of constant σ run from top to bottom. Breakdown occurs also during the run-up and it is indicated by the arrow. Contour values increase from dark blue to white.

3 A solution for merging solitary pulses

The linearity of equation (2.8) means its solution can be given as a sum of solitary-pulse solutions. Thus we analyse a multiple-solitary-pulses solution given by:

$$\begin{aligned}\phi &= \sum_{j=0}^N \phi_j \quad (3.27) \\ &= \sum_{j=0}^N -\frac{32i}{3} \int_{-\infty}^{\infty} \operatorname{cosech}(\beta_j k) \frac{J_0(k\sigma/2) e^{ik\vartheta_j}}{J_0(2k) - iJ_1(2k)} dk\end{aligned}$$

where $\vartheta_j = X_j - 1 + \lambda/2$, $\beta_j = \pi/2\xi_j$ and $\xi_j = (3A_j/4)^{1/2}$.

From this, the main flow properties η , u and v can be computed by means of equations (2.7c), (2.9), (2.11) and (2.16c). In this section we introduce and characterize the solution for multiple-solitary-pulses. The main aspects concern the solution validity (i.e. define the condition for its breakdown), the intensification of the run-up because of the merging of two or more pulses and the eventual groupiness of the pulses. The last two aspects have been analysed by properly ‘tuning’ the only two free parameters which characterize our solution i.e. the pulse amplitude A and the separations $\Delta X = X_i - X_j$ of two initially contiguous pulses. Our interest is illustrating the run-up properties rather than tabulating the solution, hence we choose to discuss a few interesting test cases.

3.1 The breakdown condition

Here we assess the conditions for which the multiple-solitary-pulses solution does not break down. It is known (e.g. SY87 and BP) that the hodograph transformation $(\sigma, \lambda) \rightarrow (x, t)$ becomes singular close to the shoreline $\sigma = 0$. This has been confirmed by the simple exercise of numerically computing the integrals involved in the expression for \mathcal{J} all over the domain of interest.

Under the above assumption we derive an analytical condition for the pulses amplitudes and relative distances among the centres of the pulses such that no breakdown occurs. It is easy to show that

$$\lim_{\sigma \rightarrow 0} u(\sigma, \lambda) = \frac{4i}{3} \int_{-\infty}^{\infty} k^2 \operatorname{cosech}(\beta k) \frac{e^{ik\vartheta_j}}{J_0(2k) - iJ_1(2k)} dk \quad (3.28)$$

which does not depend on σ . Hence, in the limit $\sigma \rightarrow 0$:

$$\mathcal{J} \approx -\frac{1}{4} \left(u_\lambda - \frac{1}{2}\right)^2 \quad (3.29)$$

and the Jacobian, which for pulse amplitudes small enough is negative all over the domain $\sigma > 0$, can only vanish inside the domain for $u_\lambda \geq 1/2$. The transformation is then regular for

$u_\lambda < \frac{1}{2}$ where

$$u_\lambda = -\frac{2}{3} \int_{-\infty}^{\infty} k^3 \operatorname{cosech}(\beta k) \frac{e^{ik\vartheta}}{J_0(2k) - iJ_1(2k)} dk. \quad (3.30)$$

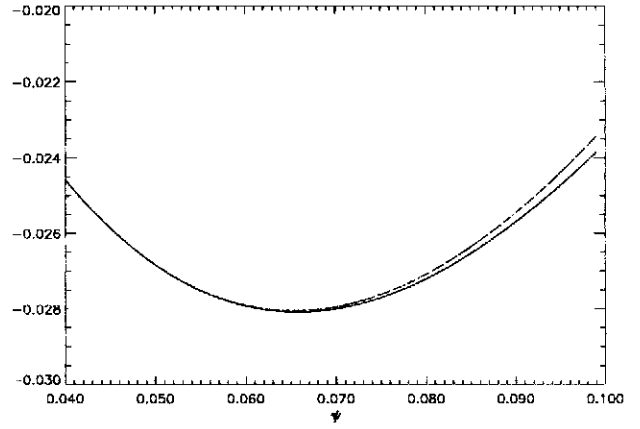


Fig. 4. Behaviour of $\sum_{m=1}^M (-1)^m m^{7/2} \Psi^m$ for $M = 5$ (solid line), $M = 50$ (dashed line) and $M = 100$ (dot-dashed line).

Following the procedure given in SY87, the function u_λ can be computed analytically by means of Cauchy’s integral formula. This is possible due to the analyticity of the integrands as discussed in Synolakis (1988). Further, for large values of ξ , each term of the resulting Laurent series can be replaced by its asymptotic form. The condition for the transformation to be regular in case of multiple-solitary-pulses is then:

$$-12(\pi\sqrt{3})^{1/2} \sum_{j=1}^N A_j^{9/4} \sum_{m=1}^{\infty} (-1)^m m^{7/2} e^{-2m\xi_j \chi_j} < \frac{1}{2} \quad (3.31)$$

where $\chi_j = X_j + 1 + \lambda/2$.

This is the most general, although rather complicated, relation which combines both A_j s and χ_j s to represent the breakdown criterion for the multiple-solitary-pulse solution. It can also be rewritten as:

$$\begin{aligned}-12(\pi\sqrt{3})^{1/2} \sum_{j=1}^N A_j^{9/4} \Sigma_j &< \frac{1}{2} \\ \text{where } \Sigma_j &= \sum_{m=1}^{\infty} (-1)^m m^{7/2} e^{-2m\xi_j \chi_j}. \quad (3.32)\end{aligned}$$

However, it is possible to obtain a pair of much simpler (although weaker) constraints for the A_j s and χ_j s separately. The first step is to notice that

$$\text{Min} \left(\sum_{m=1}^{\infty} (-1)^m m^{7/2} \Psi^m \right) = \Sigma_{\min} = -0.0285 \quad (3.33)$$

for $\Psi = \Psi_{\min} = 0.0653$. This is also illustrated by figure 4 which shows that convergence is achieved for $M = 50$ where M is used as an upper limit for the index m of Σ_{\min} .

Hence, for suitable values of χ_j , (i.e. suitable values of $\Psi_j = e^{-2\xi_j \chi_j}$) it is possible to minimize the sum Σ_j for each j . This assumption gives a first constraint for the χ_j s i.e. for the X_j s:

$$\begin{aligned}-2\xi_j \chi_j &= \ln(\Psi_{\min}) \\ \Rightarrow X_j &= -\left(1 + \frac{\lambda}{2} + \frac{\ln(\Psi_{\min})}{\sqrt{3}A_j}\right). \quad (3.34)\end{aligned}$$

Once known the initial position and height of a solitary pulse (for simplicity labelled by $j = 1$) it is possible to compute the initial position of any other solitary pulse (labelled by j) according to the simple formula:

$$X_j = X_1 + \frac{\ln(\Psi_{min})}{\sqrt{3}} \left(\frac{1}{\sqrt{A_1}} - \frac{1}{\sqrt{A_j}} \right). \quad (3.35)$$

Note that $A_1 = A_j$ implies that $X_j = X_1$ in order to minimize the sums Σ_j .

The main constraint for the regularity of the solution is derived by equation (3.31) where we substitute Σ_{min} for the second sum:

$$-12(\pi\sqrt{3})^{1/2}\Sigma_{min} \sum_{j=1}^N A_j^{9/4} < \frac{1}{2}. \quad (3.36)$$

This reduces to the condition:

$$\sum_{j=1}^N A_j^{9/4} < -\frac{1}{24(\pi\sqrt{3})^{1/2}\Sigma_{min}} \approx 0.627. \quad (3.37)$$

Note that this constraint reduces to the criterion of equation (2.25) as for $N = 1$:

$$A_1^{9/4} < 0.627 \implies A_1 < (0.627)^{4/9} = 0.81. \quad (3.38)$$

The weak formulation of the breakdown criterion is such that equation (3.37) can be used only if the pulses peaks are separated by a distance given by (3.35).

On the other hand, if condition (3.35) is not satisfied by a given initial distribution of pulses, the contributions of the Σ_j s cannot be minimized and the strong version of the constraint (3.37) must be satisfied for the transformation not to break down. From equation (3.31) this can be given as:

$$\sum_{j=1}^N A_j^{9/4}\Sigma_j < -\frac{1}{24(\pi\sqrt{3})^{1/2}} \quad (3.39)$$

and, given the initial pulses distribution, can only be computed by numerical means.

3.2 The run-up intensification

One of the most important aspects of the analysis of waves meeting in shallow waters is the assessment of the extent of the run-up. In particular we want to investigate any large intensifications due to the merging of solitary pulses. In other words we want to show that it is possible to obtain a run-up larger than that of the pulse of limiting amplitude ($A = 0.81$) by superposing some solitary pulses of smaller amplitude. The interaction we consider can be defined according to Miles (1977) as 'strong' because it is a long-time interaction between pulses travelling in the same direction.

Note that in order to compare the solution for merging pulses to that of the limiting pulse centered at $X = 4$ we consider the N -pulses solution having pulses centered inside the region $1 \leq X \leq 4$.

A large number of tests have been run in order to achieve this result which is illustrated in figure 5. At the top left corner (figure 5a) we find the free surface elevation pattern of the pulse of limiting amplitude. A similar pattern is shown by figure 5b for a pulse of amplitude $A = 0.5$. This shows a run-up of about a half of that of the limiting pulse. By properly adjusting the distances between the pulses and their amplitudes we achieved a multiple-solitary-pulse made of $N = 4$ equispaced pulses which does not break down and is characterized by a run-up about 30% larger than that of the limiting pulse (see figure 5c). A pulses amplitude has been used of $A = 0.5$ and the pulses initial positions are respectively at $X = 1, 2, 3, 4$. Note that, although the run-up pattern is similar to that of a single pulse, figures 5b, 5c and 5d refer to multiple-solitary-pulses i.e. to initial conditions such that $N = 4$ different pulses are superposed each with a different centre X_j . In section 3.3 a detailed analysis is reported in order to establish a criterion which relates the run-up shape to the pulses initial separation.

Although it is possible to achieve a similar result by a different combination of amplitudes and positions we find it is not trivial to 'tune' these properties in order to get a large run-up with no breakdown. For example breakdown occurs by superposing in the region $1 \leq X \leq 4$ two or more pulses of amplitude $A = 0.6$ or larger. This justifies the choice of describing multiple-solitary-pulses by using a maximal amplitude of $A = 0.5$.

A better result can be achieved by superposing a large number of pulses of small amplitude. Figure 5d shows a run-up pattern very similar to that of figure 5c; however, this has been achieved by using $N = 7$ pulses of amplitude $A = 0.25$ centered at positions equispaced of $\Delta X = 0.5$ seaward of $X = 1$. Comparison of the last two figures of 5 also illustrates a simple concept: *a comparatively larger run-up can be achieved by using a large number of small pulses densely distributed ($N = 7$, $A = 0.5$ and $\Delta X = 0.5$ case) than using less, larger pulses more sparsely distributed ($N = 4$, $A = 0.25$ and $\Delta X = 1.0$ case).*

A final consideration concerns the 'nonlinearity parameter' \mathcal{N} of equation (2.23). Paradoxically this decreases mainly by increasing the number of pulses considered as $\mathcal{N} = 0.30$ for the ($A = 0.50$, $N = 4$) pulses case which can be compared with both the ($A = 0.25$, $N = 7$) case ($\mathcal{N} = 0.20$) and the the ($A = 0.50$, $N = 1$) case ($\mathcal{N} = 0.40$). This is simply explained by noting that $\text{Max}(v) = \text{Max}(\eta)$ increases with N faster than $\text{Max}(\eta - v) = \text{Max}(u^2/2)$ increases with either A or N . Dependence of \mathcal{N} on the pulses separation is studied in the next section.

Note that choosing the conditions for the multiple-solitary-pulses of figure 5 we contravened equation (3.35) as we used $A_i = A_j$ with $X_i \neq X_j$. For the above cases the appropriate condition to avoid breakdown is (3.39).

3.3 Waves separation and groupiness

It is clear that if flow intensification depends on the initial spatial separation among pulse peaks ΔX it is necessary to

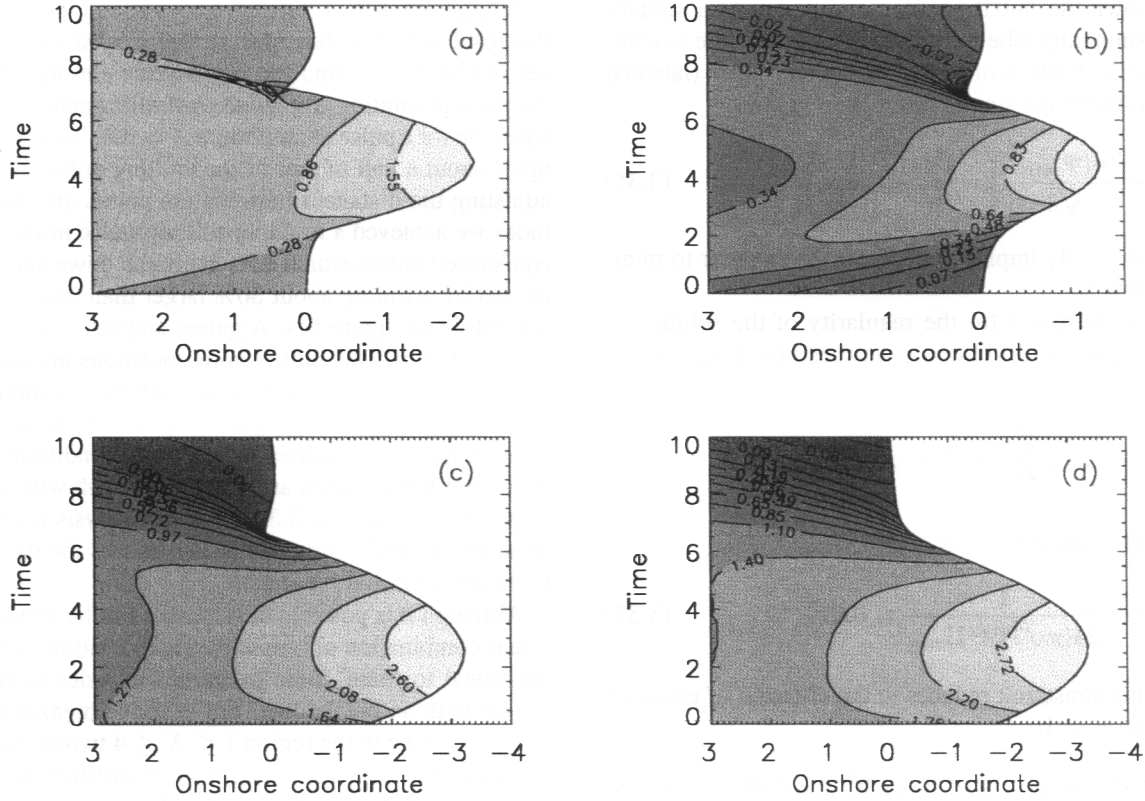


Fig. 5. The patterns of free-surface elevation for solitary pulses. (a) Single limiting pulse of ($A_1 = 0.81, X_1 = 4.$), breakdown occurs during run-down; (b) single pulse of ($A_1 = 0.5, X_1 = 4.$). (c) Multiple-solitary-pulse of $N = 4$ pulses. Each pulse has amplitude $A = 0.5$ and initial positions equispaced of $\Delta X = 1$ seaward of $X = 1$. (d) Multiple-solitary-pulse of $N = 7$ pulses. Each pulse has amplitude $A = 0.25$ and initial positions equispaced of $\Delta X = 0.5$, seaward of $X = 1$. Contour values increase from dark blue to white.

relate this distance to the already defined 'equivalent wave length' L or, better to relate important flow characteristics to the relative initial separation $\Delta X/L$.

A somehow similar analysis has been performed by Stiassnie and Peregrine (1980) in their study of a train of 'KdV-type' solitary waves (TSW) propagating in water of slowly-varying depth. They considered some aspects of the wave-wave and wave-seabed interaction in shallow waters and gave an estimate of the relative importance of the two interactions on the propagation of the train.

A simple approach is taken here in order to describe the wave-wave interaction in view of the influence on the run-up pattern. The easiest way would be to compare the separation $(u\Delta t)_{shore}$ between peaks of inundation with the largest wave length in the group (L_{max}) but often this is not significant in the very shallow water of the 'swash zone' (i.e. the inundation region). Here peaks of run-up of each wave of a group often coalesce to give one single large run-up pattern making it difficult (or impossible) to define $(u\Delta t)_{shore}$. This is particularly true when the group is made of pulses of different amplitudes.

To overcome this problem we define a 'groupiness parameter' $\mathcal{G} = \mathcal{G}(\Delta X/L)$ such that:

$$\mathcal{G} = \frac{(\mathcal{R})_{group}}{(\mathcal{R})_{pulse}} \quad (3.40)$$

where

- \mathcal{R}_{group} = largest run-up of the group;
- \mathcal{R}_{pulse} = run-up of the single largest pulse of the group.

According to this definition as regards the run-up a group of N pulses in shallow waters can be considered as made of single, non-interacting pulses for $\mathcal{G} \approx 1$ while increasing \mathcal{G} gives a measure of the increasing interaction or groupiness.

In order to keep the analysis simple we have studied two pulses interacting in shallow water in dependence of the relative initial separation $\Delta X/L$. The two functions \mathcal{N} and \mathcal{G} have been computed for different separations and the effects of increasing/decreasing amplitude have also been taken into account (parametrically). The results are reported in figure 6.

Figure 6a reveals that the nonlinearity parameter \mathcal{N} is not monotonically decreasing with the pulses separation as one might expect. Rather, there is a critical separation $(\Delta X)_c$ for which nonlinearities are minimized. This distance, which does not depend on the pulse amplitude, is found to be

$$(\Delta X)_c \approx \frac{L}{2}. \quad (3.41)$$

As $\text{Max}(\eta) = \text{Max}(v)$ steadily decreases with increasing separation the above behaviour must be due to the non-monotonic decrease of u with separation. This is better explained by referring to figure 7.

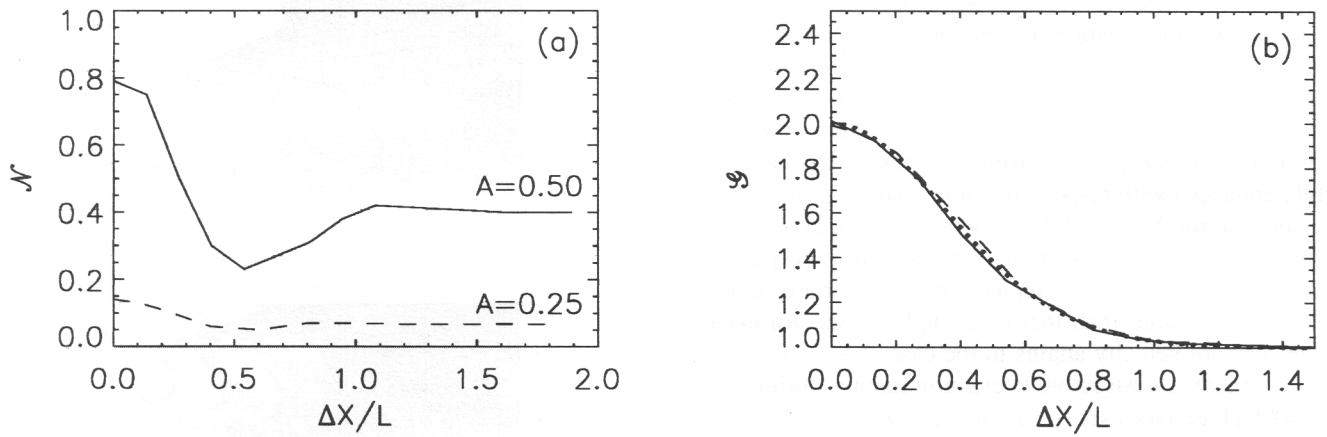


Fig. 6. Dependence of the nonlinearity parameter \mathcal{N} (figure a) and the groupiness parameter \mathcal{G} (figure b) on the relative initial pulse distance. Solid curves are for $A = 0.50$ and dashed curves for $A = 0.25$. The dotted line in figure b shows the analytical expression $\mathcal{G} = 1 + \text{sech}^8(\Delta X/L)$.

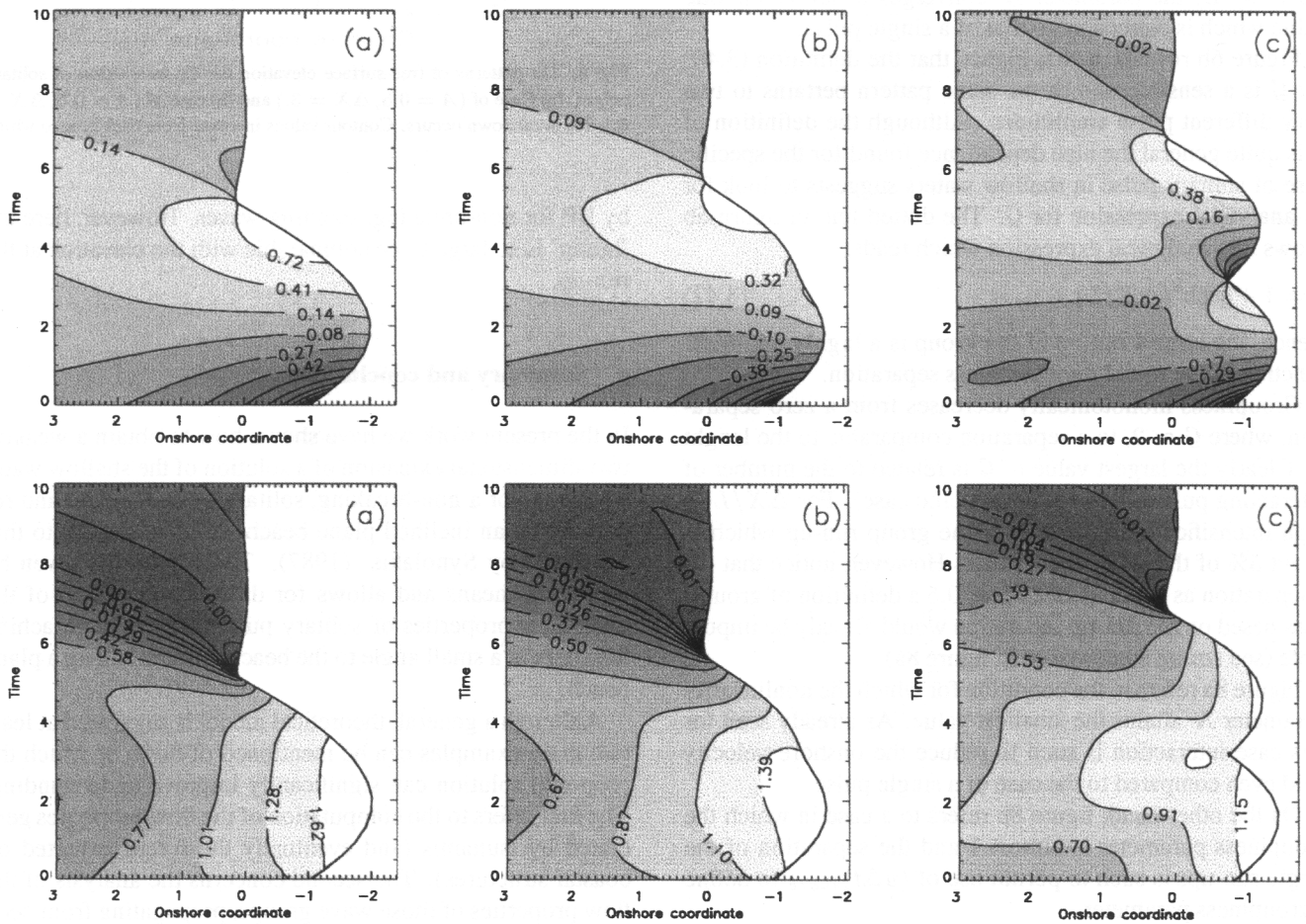


Fig. 7. Patterns of onshore (top row) and longshore velocities (bottom row) for two solitary-type pulses of amplitude $A = 0.50$. Results for three different pulse separations are reported from left to right: $\Delta X = (\Delta X)_c - 0.15L$, $(\Delta X)_c$, $(\Delta X)_c + 0.30L$

Here patterns of onshore velocity (top row) and longshore velocity (bottom row) have been reported respectively for the three pulse separations (from left to right) $\Delta X = (\Delta X)_c - 0.15L$, $(\Delta X)_c$, $(\Delta X)_c + 0.30L$ for a pulse of amplitude $A = 0.50$. Two main features can be immediately seen.

First of all for $\Delta X < (\Delta X)_c$ coalescence between the two pulses is almost perfect (figures 'a' of both rows and cases of previous section) giving a single run-up pattern in which the onshore velocity (mainly during the back-wash phase) is slightly enhanced with respect to that of a single pulse. This is not the case for $\Delta X > (\Delta X)_c$ (figures 'c' of both rows) as the run-up pattern is more similar to that of two single pulses (although separation is not complete) and the onshore velocity is slightly smaller than that of a single pulse. An even smaller onshore velocity attains to the case $\Delta X = (\Delta X)_c$ for which there is destructive interaction mainly during the back-wash phase (see case 'b' of the top row).

A second important factor is the monotonic decrease of longshore velocity with the pulse separation (see second row of figure 7). Clearly, interaction between the two pulses always increases the longshore flow.

Figure 6a also shows that for large values of separation ($\Delta X \geq L$) the parameter \mathcal{N} converges to an asymptotic value which is equivalent to that of a single pulse.

Figure 6b reveals at first glance that the definition (3.40) for \mathcal{G} is a sensible one as the same pattern pertains to two very different pulse amplitudes. Although the definition of \mathcal{G} is quite general the nice dependence found for the specific case of solitary pulse in shallow waters suggests to look for an analytical expression for \mathcal{G} . The dotted line in figure 6b shows this analytical expression which reads:

$$\mathcal{G} = 1 + \operatorname{sech}^8(\Delta X/L). \quad (3.42)$$

Hence, the largest run-up of the group is a highly nonlinear function of the initial dimensionless separation.

Groupiness monotonically decreases from a zero separation, where $\mathcal{G} \approx 2$, to a separation comparable to the length L . Clearly the largest value of \mathcal{G} is related to the number of interacting pulses (two for the specific case). For $\Delta X/L \geq 1$ an intensification is found for the group run-up which is about 5% of that of a single pulse. However, notice that for a separation as small as $\Delta X/L \approx 0.5$ a definition of groupiness based on the run-up separation would already be impossible (see strong coalescence in figure 8a).

Figure 8a refers to the condition for which the nonlinearity parameter \mathcal{N} attains the smallest value. As already seen for this case interaction is such to reduce the onshore velocity field even compared to the case of a single pulse.

On the other hand, figure 8b refers to a case in which the groupiness parameter is almost 1 and the separation of the single run-ups is such to permit use of $(u\Delta t)_{shore}$ to define a groupiness parameter.

Finally note the interesting feature of this run-up pattern which pertains to the 'hump' of free surface elevation just seaward of the run-down position (i.e. for $t \approx 4$). This is due to the interaction of the back-wash of the first pulse and the second incoming pulse. A similar pattern was already shown

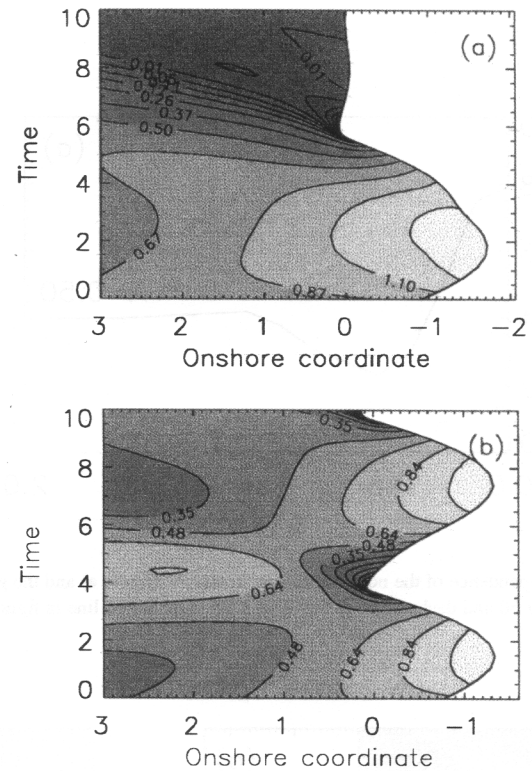


Fig. 8. The patterns of free-surface elevation for the interaction of solitary pulses. (a) Case of ($A = 0.5, \Delta X = 3.$) and (b) case of ($A = 0.5, \Delta X = 6.$). No breakdown occurs. Contour values increase from dark blue to white.

by BP for non-breaking, standing waves. However, here the 'hump' is so large to be comparable with the elevation at the run-up.

4 Summary and conclusions

In the present work we have shown how to obtain a weakly-two-dimensional extension of a solution of the shallow water equations for a non-breaking, solitary pulse incident and reflecting on an inclined plane beach which is similar to that suggested by Synolakis (1987). The solution is given by analytical means and allows for direct computation of the main flow properties of solitary pulses which, approaching the shore at a small angle to the beach normal, run up a plane beach.

Although a general, theoretical model is suggested at least two main examples can be mentioned of flows of which the proposed solution can significantly improve understanding. The first refers to the computation of the flow properties generated by tsunamis (and eventually the forces exerted on coastal structures). The second concerns the analysis of the flow properties of those wave groups, propagating from deep to shallow waters, in which the primary waves, modulated by a longer underlying modulation, behave like solitary pulses. Depending on the group characteristics (groupiness) these can either be considered as single-solitary-pulses for which a well-defined run-up/back-wash pattern is identified or they

can interact as a multiple-solitary-pulse solution.

For a single-solitary-pulse, the longshore velocity v is very similar to the free-surface elevation η for a large portion of the considered domain. However, close to the shoreline, nonlinear contributions expressed as function of the onshore velocity u can be regarded as perturbations of the patterns of η . Intensity of nonlinearities have been measured in terms of a nonlinearity parameter \mathcal{N} . A pulse of limiting amplitude has been introduced such that breakdown of the solution occurs for amplitudes larger than $A = 0.81$.

Breakdown of the solution is analysed for a multiple-solitary-pulses solution. A strong condition is given which couples information on both pulses amplitudes and distances. An easier (but weaker) version of the criterion is given in terms of a pair of decoupled formulae one for the pulses amplitudes and the second for their initial positions. These conditions can be used to assess the possible interaction conditions for a group of solitary waves which, running up a plane beach, can interact both with each other and with the swash motion from previous waves.

Run-up intensification due to merging in shallow waters of solitary-type pulses has been analysed. It is found that under suitable conditions such that $\Delta X < L/2$ it is possible to achieve a run-up larger than that of a limiting pulse without reaching breakdown of the solution.

Influence of the initial relative pulse separation on run-up patterns has been studied by introducing a 'groupiness parameter' \mathcal{G} . It is shown that the definition is sound and it is found that for the specific case of solitary pulses it is possible to give an analytic expression for \mathcal{G} . Finally, it is shown that nonlinearities which characterize the solution can be minimized by putting $\Delta X = L/2$ the initial pulses separation.

Since the presented solution for the run-up of non-breaking, multiple-solitary-pulse is an 'easy-to-use' tool for predicting the inundation properties of a train of solitary waves research work is in progress for applying the solution to the modelling of extreme wave trains which are to be built on the basis of both experimental observation and of quasi-deterministic theories of sea wave groups. Clearly the above analytical approach is not to be applied to breaking waves. In that case results of run-up intensification and wave separation are expected to differ from those here described.

A second field of application of the weakly-two-dimensional solution for solitary-type pulses could be the estimation

of the forces exerted in the longshore direction on coastal structures.

Acknowledgements. The author is grateful for several useful discussions with Professor C.E. Synolakis and for the interesting suggestions he made. Thanks are also extended to Professors G. Seminara and P. Blondeaux for carefully and critically reading the revised version of the manuscript.

References

- Barnes, T. C. D. and Peregrine, D. H., Wave groups approaching a beach: full irrotational flow computation. *Proc. Coastal Dynamics '95-ASCE*, 1, 116–127, 1995.
- Brocchini, M. and Peregrine, D. H., Integral flow properties of the swash zone and averaging. *J. Fluid Mech.*, 317, 241–273, 1996.
- Carrier, G. F., Gravity waves of water of variable depth. *J. Fluid Mech.*, 24, 641–659, 1966.
- Carrier, G. F. and Greenspan, H. P., Water waves of finite amplitude on a sloping beach. *J. Fluid Mech.*, 4, 97–109, 1958.
- Carrier, G. F. and Noiseux, C. F., The reflection of obliquely incident tsunamis. *J. Fluid Mech.*, 133, 147–160, 1983.
- Golinko, V. and Pelinovsky, E., Long wave runup on a beach in a channel of arbitrary cross-section. *Soviet Meteorology and Hydrology*, 9, 107–112, 1988.
- Kobayashi, N., DeSilva, G. S. and Watson, K. D., Wave transformation and swash oscillation on gentle and steep slopes. *J. Geophys. Res.*, 94, 951–966, 1989.
- Liu, P. L.-F., Synolakis, C. E. and Yeh, H. H., Report on the International Workshop on Long wave Run-up. *J. Fluid Mech.*, 229, 675–688, 1991.
- Meyer, R. E. and Taylor, A. D., Run-up on beaches. In *Waves on beaches and resulting sediment transport* (ed. R. E. Meyer). Academic Press, New York, 1972.
- Miles, J. W., Obliquely interacting solitary waves. *J. Fluid Mech.*, 79, 157–169, 1977.
- Peregrine, D. H., Equations for water waves and the approximations behind them. In *Waves on beaches and resulting sediment transport* (ed. R. E. Meyer). Academic Press, New York, 1972.
- Ryrie, S. C., Longshore motion generated on beaches by obliquely incident bores. *J. Fluid Mech.*, 129, 193–212, 1983.
- Synolakis, C. E., The run-up of solitary waves. *J. Fluid Mech.*, 185, 523–555, 1987.
- Synolakis, C. E., On the roots of $f(z) = J_0 - iJ_{n+1}$. *Q. Appl. Math.*, 46, 105–107, 1988.
- Shen, M. C. and Meyer, R. E., Climb of a bore on a beach. Part 3. Run-up. *J. Fluid Mech.*, 16, 113–125, 1963.
- Stassnie, M. and Peregrine, D. H., Shoaling of finite-amplitude surface waves on water of slowly-varying depth. *J. Fluid Mech.*, 97, 783–805, 1980.
- Voit, S. S., Tsunamis. *Ann. Rev. Fluid Mech.*, 19, 217–236, 1987.
- Watson, G., Barnes, T. C. D. and Peregrine, D. H., The generation of low frequency waves by a single group incident on a beach. *Proc. 24th Internat. Conf. Coast. Engng*, 1, 776–790, 1994.